

RESEARCH ARTICLE

Intravital Imaging of Tumor Apoptosis with FRET Probes During Tumor Therapy

Feifan Zhou,¹ Da Xing,¹ Shengnan Wu,¹ Wei R. Chen^{1,2}

¹MOE Key Laboratory of Laser Life Science and Institute of Laser Life Science, South China Normal University, Guangzhou, 510631, China

²Biomedical Engineering Program, Department of Engineering and Physics, College of Mathematics and Science, University of Central Oklahoma, Edmond, OK, 73034, USA

Abstract

Purpose: The aim of the study is to dynamically and non-invasively monitor the apoptosis events *in vivo* during photodynamic therapy (PDT) and chemotherapy.

Procedures: A FRET probe, SCAT3, was utilized to determine activation of caspase-3 during tumor cell apoptosis in mice, induced by PDT, and cisplatin treatments. Using this method, dynamics of caspase-3 activation was observed both *in vitro* and *in vivo*.

Results: Analysis of the fluorescent missions from tumor cells indicated that the caspase-3 activation started immediately after PDT treatment. In contrast, the caspase-3 activation started about 13 and 36 h after cisplatin treatment *in vitro* and *in vivo*, respectively.

Conclusions: FRET could be used effectively to monitor activation of caspase-3 in living organism. This method could be used to provide rapid assessment of apoptosis induced by anti-tumor therapies for improvement of treatment efficacy.

Key words: Apoptosis, FRET, SCAT3, Caspase-3, PDT, Cisplatin

Introduction

Apoptosis is an important cellular event that plays a key role during treatment of many diseases [1, 2]. A method of monitoring apoptosis in a living organism could be used to assess therapeutic effects. Imaging apoptosis may involve using different imaging modalities, ranging from scintigraphy to magnetic resonance imaging [3–6] to detect one or more of a large number of markers associated with apoptosis.

The use of biosynthetic fluorescent sensors is an important approach for imaging apoptosis *in vivo*. Recently reported fluorescent sensors for assessing anti-tumor efficacies were genetically encoded optical probes [7, 8]. Cy5.5-AnnexinV probe was used to monitor the externalization of aminophospholipids normally residing on the cytoplasmic leaflet of plasma membrane during earliest apoptosis [9, 10]. ICE-NIRF probe was used to detect caspase-1 activation

[11] and TcapQ647 probe was used to detect caspase-3 activation during apoptosis [12]. In addition, fluorescent proteins (FP)-based biosensors, especially those based on Förster resonance energy transfer (FRET), could report on Ca²⁺ dynamics and caspase-3 activation [13–15]. The presence of apoptotic cells *in vivo* is usually transient, *i.e.*, there is a limited time period between the onset of apoptosis and the eventual cell removal [16]. Therefore, the detection of apoptosis ideally should be accomplished using a high-affinity and stable marker with a fast response to apoptosis.

FRET has been widely used to study protein–protein interactions in living cells [17–19]. Specifically, FRET has been used to detect apoptotic signals that involve PKC activation, Bid cleavage, caspase-3 activation [20–24], and change of Ca²⁺ level [19, 25, 26]. Takemota et al. [27] has constructed a FRET probe, SCAT3, which consists of a donor (enhanced cyan fluorescent protein, ECFP) and an acceptor (Venus, a mutant of yellow fluorescent protein). The linking sequence contains the caspase-3 cleavage site DEVD [28]. The activation of caspase-3 leads to the

cleavage of the linker, thus effectively reducing the FRET. Using FRET probe SCAT3, the spatiotemporal dynamics of caspase-3 activity could be monitored in real-time [27].

Our previous study has proven that FRET can be used to investigate caspase-3 activation in single cells [29, 30]. In the current study, we investigated the dynamics of caspase-3 activation during tumor cell apoptosis induced by PDT and cisplatin in cell culture and in animals. Our results demonstrate the feasibility of FRET-based assays for real-time visualization of cell apoptosis in living tissues.

Materials and Methods

Chemicals and Plasmids

The following chemicals and fluorophore probes were used: photosensitizer Photofrin (QLT Phototherapeutics, Vancouver, BC, Canada) for PDT treatment, cisplatin (Sigma, St Louis, MO, USA) for chemotherapy treatment, pentobarbital sodium (40 mg/kg, Sigma) to anesthetize animals, *in situ* apoptosis detection kit (TUNEL) (R&D Systems, Minneapolis, MN, USA) to detect DNA fragmentation in tissue, and Hoechst 33325 (1 μ g/ml, Sigma) to study the nuclear morphology of cells. In addition, we used Lipofectin reagent (Invitrogen life technologies, USA) to transfect plasmid DNA into tumor cells and G418 antibiotic (0.8 mg/ml, Sino-American Biotec, China) to screen the cells stably expressing reporter SCAT3. pSCAT3 was a gift from Dr. Masayuki Miura [27].

Cell Culture

The human lung adenocarcinoma cell line (ASTC-a-1) was cultured in DMEM supplemented with 15% fetal calf serum, penicillin (50 U/ml), and streptomycin (50 μ g/ml) in 5% CO₂, 95% air at 37°C in humidified incubator.

Tumor Model

ASTC-a-1 cells with and without SCAT3-expression were used to establish tumors in female Balb/c nude mice. Cells (2×10^6) in a 100 μ l solution were injected into the flank region of mice (three groups; $n=4$ animals/group). PDT and cisplatin treatments were performed on day 7 after the inoculation of tumor cells, when tumors in mice reached a size of 3–4 mm.

Photodynamic Therapy and Cisplatin Treatments of Tumor Cells in Tissue Culture

For PDT treatment, cells (1×10^5) growing in 35 mm Petri dishes were incubated in the dark with Photofrin (3 μ g/ml in complete growth medium) for 20 h, rinsed with PBS, and exposed to light with a dose of 5 J/cm² (10 mW/cm²). The light source was a He-Ne laser (HN-1000, Guangzhou, China; 632.8 nm). The observation of the PDT-treated cells started immediately after the laser irradiation. For chemotherapy, cisplatin in aqueous solution was mixed with cells (1×10^5) growing in 35-mm Petri dishes with a final cisplatin concentration of 20 μ M. The observation of the cells started immediately after the cisplatin treatment. Cells (1×10^5) growing in 35-mm Petri dishes without any treatment was used as the control.

Photodynamic Therapy and Cisplatin Treatments of Mouse Tumors

Photofrin was administered intraperitoneally (i.p.) at a dose of 10 mg/kg, 24 h before illumination with the 633 nm light (day 7 after inoculation with tumor cells). The light was delivered to tumors on day 8 using a fiberoptic light delivery system. The power density at the illumination area, which encompassed the tumor and 0.5–1 cm of the surrounding skin, was 40 mW/cm². The total light dose delivered to each tumor was 120 J/cm². During the light irradiation, mice were anesthetized with an i.p. injection of pentobarbital sodium and were restrained in a specially designed holder.

In chemotherapy, starting on day 7 after inoculation with tumor cells animals received daily i.p. injection of cisplatin (10 mg/kg) in 100 μ l volumes for five consecutive days. Immediately after the last cisplatin injection, mice were anesthetized and restrained for imaging analysis with a fluorescence stereo microscope.

Hoechst 33325 and TUNEL Staining

To assess changes of nuclear morphology in cells during apoptosis, cells (1×10^5) were cultured in 35-mm glass bottomed dishes. Three hours after PDT treatment and 20 h after cisplatin treatment, the cells were stained with Hoechst 33325 for 10 min at room temperature and washed twice with PBS. The cell samples were visualized under a Nikon fluorescence microscope with a hydrargyrum lamp. Hoechst 33325 was excited by light through a 330–380-nm band-pass filter and emitted light was detected through a 450–490-nm band-pass filter.

Individual tumors were excised 6 h after PDT treatment and 60 h after cisplatin treatment. The tumor samples were placed immediately in Tris-buffered zinc fixative [0.1 M Tris-HCl buffer (pH 7.4) containing 3.2 mM calcium acetate, 22.8 mM zinc acetate, and 36.7 mM zinc chloride] for 6–18 h, transferred to 70% ethanol, dehydrated, and embedded in paraffin. Cryostat sections (10 μ m thick each) were cut from each tumor sample. TUNEL staining was performed for the tumor sections. DNA fragmentation was detected by terminal deoxynucleotide transferase-based, *in situ* apoptosis detection kit (TUNEL), following the manufacturer's instructions. Biotinylated nucleotides incorporated into the DNA fragments were detected using a streptavidin-fluorescein conjugate, which was excited with the 488 nm line of an Ar-laser. Fluorescence emission was recorded using a 500–550-nm band-pass filter.

FRET Reporters

A genetic FRET reporter, SCAT3, was used to monitor caspase-3 activity. This reporter consists of a donor cyan fluorescent protein (ECFP) and an acceptor Venus (a mutant of yellow fluorescent protein). The donor and the acceptor are linked with a caspase-3 recognition and cleavage sequence, DEVD. Activation of caspase-3 leads to the cleavage of the linker, thus effectively reducing the FRET. Therefore, a decrease in FRET represents the activation of caspase-3 in cells.

FRET Analysis

FRET in cells was performed on a commercial Laser Scanning Microscope (LSM510/ConfoCor2) combination system (Zeiss, Jena, Germany) with an inverted microscope. For excitation, the

458 nm line of an Ar-Ion Laser was attenuated with an acousto-optical tunable filter, reflected by a dichroic mirror (main beam splitter HFT458) and focused through a Zeiss Plan-Neofluar 40 \times /1.3 NA Oil DIC objective onto the sample. The fluorescent emission was split by a second dichroic mirror (secondary beam splitter NFT515) into two separate channels: the 470–500-nm band-

pass (ECFP channel) and the 530-nm long-pass (Venus channel). For intracellular measurements, the regions of interest (ROIs) were chosen in the LSM images. To quantify the results, the average emission intensities of ECFP and Venus from the ROIs were processed with the Zeiss Rel3.2 image processing software (Zeiss, Germany).

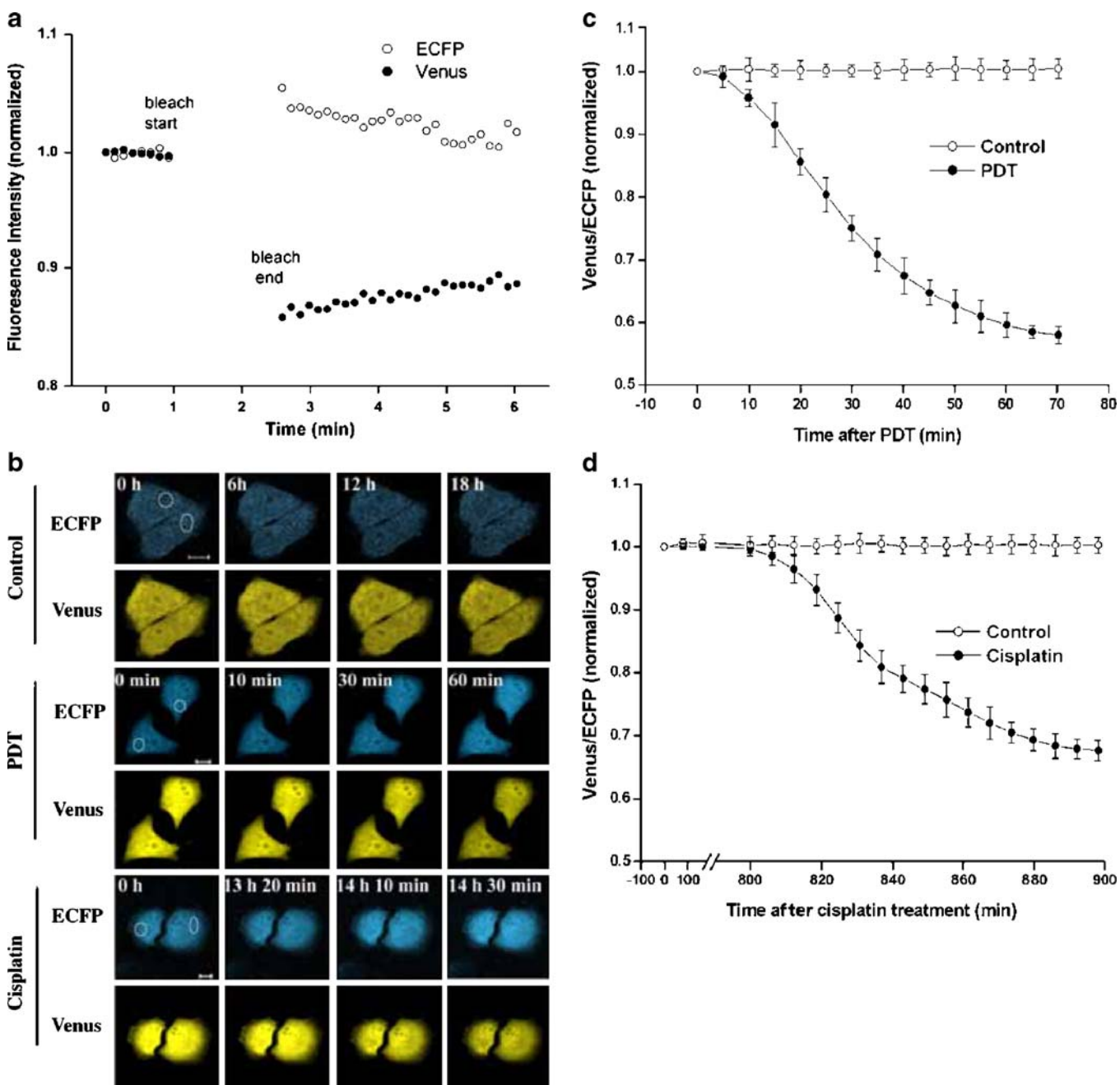


Fig. 1. **a** Quantitative analysis of ECFP and Venus fluorescence following repeated scanning. FRET decreases significantly due to bleaching of Venus. Venus was bleached using the Ar 514 nm line. **b** Fluorescent images of ECFP and Venus of ASTC-a-1 cells after PDT or cisplatin treatment. For controls, the SCAT3-expressing ASTC-a-1 cells were exposed to room air and kept at 37 $^{\circ}$ C for 18 h. For PDT treatment, the SCAT3-expressing ASTC-a-1 cells were exposed to 3 μ g/ml Photofrin for 20 h in the dark, and then treated with 633 nm light (5 J/cm 2). For chemotherapy, cisplatin in aqueous solution was mixed with cells (1×10^5) growing in 35 mm Petri dishes with a final cisplatin concentration of 20 μ M. After treatment, cells were observed using a confocal microscope. Bar=10 μ m. **c** and **d** Time course of Venus/ECFP fluorescence intensity ratio obtained from four regions of interest (ROIs) of the cells in tissue culture after PDT treatment (**c**) and cisplatin treatment (**d**), mean \pm SD, $n=4$.

FRET *in vivo* was measured on the stage of a stereo microscope (Lumar V12, Zeiss, Jena Germany) with a hydrargyrum lamp (HBO100) as light source. After the PDT or cisplatin treatment, mice were anesthetized with pentobarbital sodium and were restrained in a specially designed holder for imaging analysis with a fluorescence stereo microscope. The light beam through a 436/20-nm band-pass filter was used to excite the fluorescent probes. The fluorescent emission was recorded through two separate channels: the 480/40-nm band-pass channel (for ECFP) and the 535/30-nm band-pass channel (for Venus). To quantify the results, the average emission intensities of ECFP and Venus from the ROIs were processed with Axiovision 4.5 software (Zeiss, Germany). For the analysis of fluorescent emission from tumors in animals, four ROIs were selected. In each ROI the Venus/ECFP ratio at each designated time was calculated and the ratios were normalized to unity at zero time. Then, the normalized ratios from all four regions were averaged.

Results

FRET Efficiency of SCAT3

Acceptor bleaching experiments were carried out to assess the sensitivity of the FRET probes. The acceptor fluorophore Venus was selectively bleached by repeated scanning of the target cell area with the Ar 514 nm line. Upon bleaching there was a marked decrease in the acceptor fluorescence (Venus), which coincided with an increase in the donor fluorescence (ECFP) because of the inability of the acceptor to accept energy from the donor after bleaching (Fig. 1a). Therefore the increase of ECFP fluorescence upon Venus bleaching confirmed FRET between the two fluorescent proteins in the SCAT3-transfected cells.

Real-time Detection of Caspase-3 Activation During Apoptosis of Tumor Cells in Tissue Culture

FRET imaging was used to determine the dynamics of caspase-3 activation in SCAT3-expressing ASTC-a-1 cells after PDT and cisplatin treatments. ECFP and Venus fluorescent images were obtained from SCAT3-expressing cells after the treatment (Fig. 1b). The fluorescence intensity of ECFP increased while that of Venus decreased under either PDT or cisplatin treatment. The time courses of the Venus/ECFP fluorescence intensity ratio obtained from four regions of interest (ROIs) are shown in Fig. 1c and d. After PDT treatment, the ratio decreased immediately, and reached a stable level after about 60 min (Fig. 1c). After the administration of cisplatin, the ratio remained constant for approximately 800 min, then decreased gradually, and reached a stable level after about 900 min (Fig. 1d). For the control group, ECFP and Venus fluorescent emissions and Venus/ECFP fluorescence intensity ratio remained unchanged during the entire observation period, as shown in Fig. 1b, c, and d. These results demonstrated that the intracellular caspase-3 was activated to cleave the linker of SCAT3, DEVD, thus disrupting the FRET during apoptosis induced by PDT or cisplatin.

Photodynamic Therapy and Cisplatin Treatments Induced Apoptosis

To confirm that PDT or cisplatin treatment could effectively induce apoptosis in ASTC-a-1 cells, Hoechst 33325 staining was used. Three hours after PDT treatment (5 J/cm^2 , $3 \mu\text{g/ml}$ Photofrin) and 20 h after cisplatin treatment ($20 \mu\text{M}$),

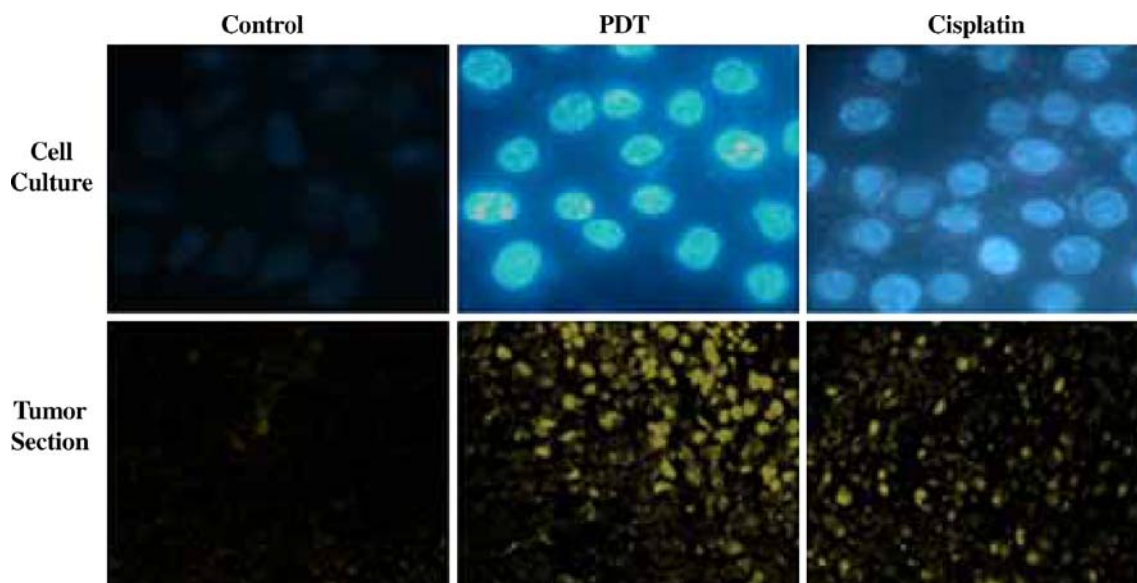


Fig. 2. Photodynamic therapy and cisplatin treatment induced apoptosis. For cells in culture, Hoechst 33325 staining was performed 3 h after PDT treatment and 20 h after cisplatin treatment (*upper panel*). For tissue sections from mouse tumors, TUNEL staining was performed 6 h after PDT treatment and 60 h after cisplatin treatment (*lower panel*). The fluorescent emissions from tumor cells treated by PDT and cisplatin indicate apoptosis.

Hoechst 33325 staining showed morphologically the occurrence of induced apoptosis in cell culture (Fig. 2, upper panel).

To validate that the treatment of PDT and cisplatin of selected doses could effectively induce tumor cell apoptosis in mice, we examined tumor sections by TUNEL staining. The tumor sections were obtained 6 h after PDT treatment (120 J/cm^2 at 40 mW/cm^2 , 10 mg/kg Photofrin) or 60 h after cisplatin treatment (10 mg/kg). TUNEL staining clearly showed morphologically the induced apoptosis in mouse tumor (Fig. 2, lower panel).

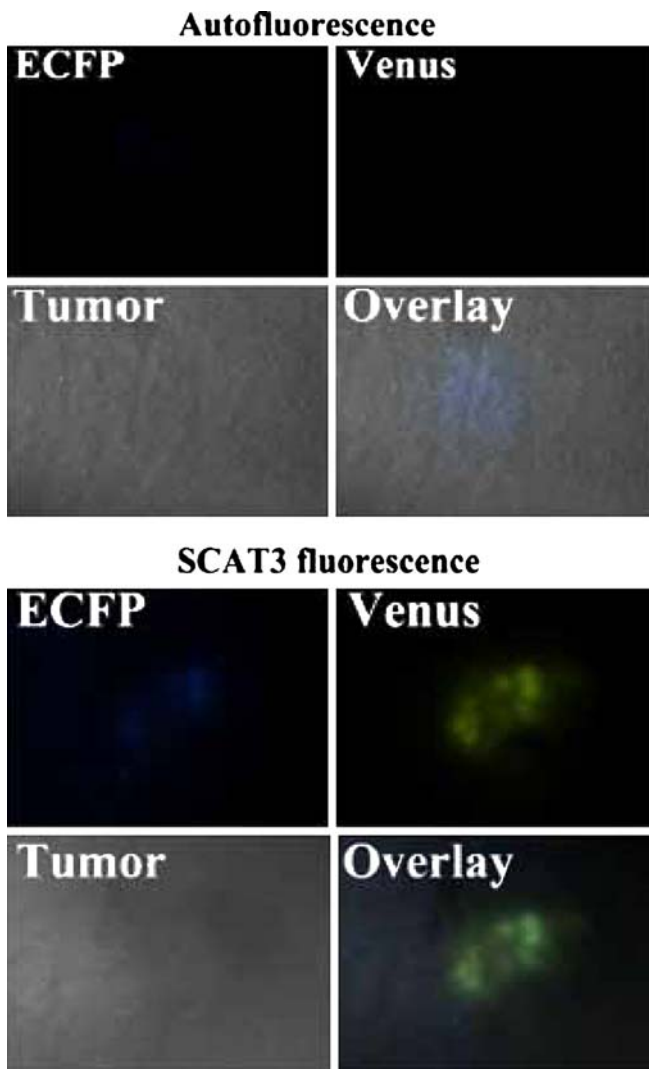


Fig. 3. Fluorescent emissions of ECFP and Venus from a mouse tumor sample, 7 days after inoculation of tumor cells with and without transfection of the SCAT3 probes, observed with a fluorescence stereo microscope. The tumor cells without SCAT3 shows weak fluorescent emission (*top panel*), while the tumor transfected by SCAT3 shows strong fluorescent emission (*bottom panel*). These results indicate that the fluorescent emission is indeed from the transfected tumor cells, not from the cell autofluorescence.

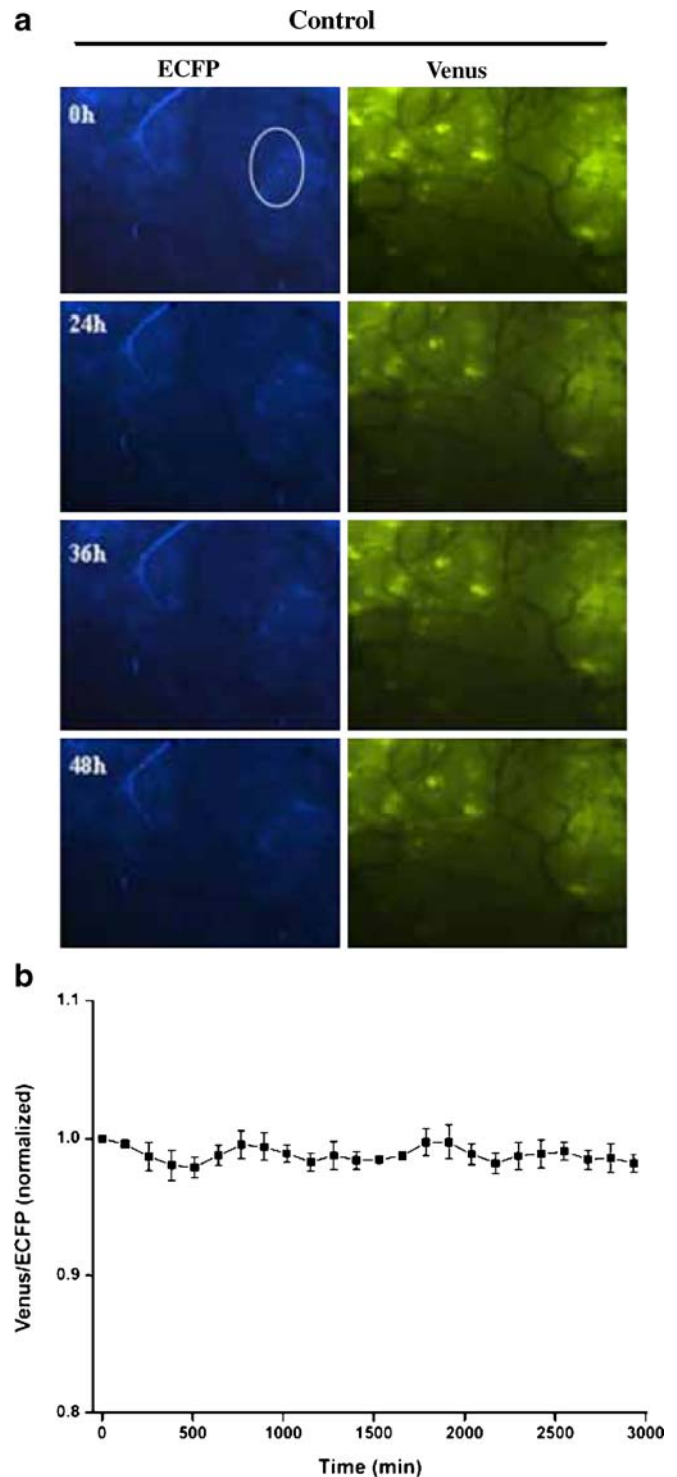


Fig. 4. The stability of FRET signals in a control mouse tumor, observed by the fluorescence stereo microscope. **a** Fluorescent images of ECFP and Venus from a mouse tumor without treatment at 0, 24, 36, and 48 h, starting on day 7 of inoculation of tumor cells. **b** Time course of Venus/ECFP fluorescence intensity ratio obtained from four ROIs of the control mouse tumor. The fluorescent images and intensities of ECFP and Venus emission were acquired with a fluorescence stereo microscope, starting on day 7 after inoculation with tumor cells stably expressing SCAT3.

Fig. 5. Dynamics of caspase-3 activation in a mouse tumor after PDT treatment. **a** Fluorescent images of ECFP and Venus from a mouse tumor at 0, 60, 90, and 120 min after PDT treatment. **b** Time course of the Venus/ECFP fluorescence intensity ratio obtained from four ROIs of the mouse tumor after PDT treatment. On day 7 after inoculation with tumor cells stably expressing SCAT3, Photofrin was administered i.p. with a dose of 10 mg/kg. The tumor was illuminated with 633 nm light (120 J/cm^2 at 40 mW/cm^2) 24 h later. The fluorescent images and intensities of ECFP and Venus emission were acquired by the fluorescence stereo microscope, immediately after the laser irradiation.

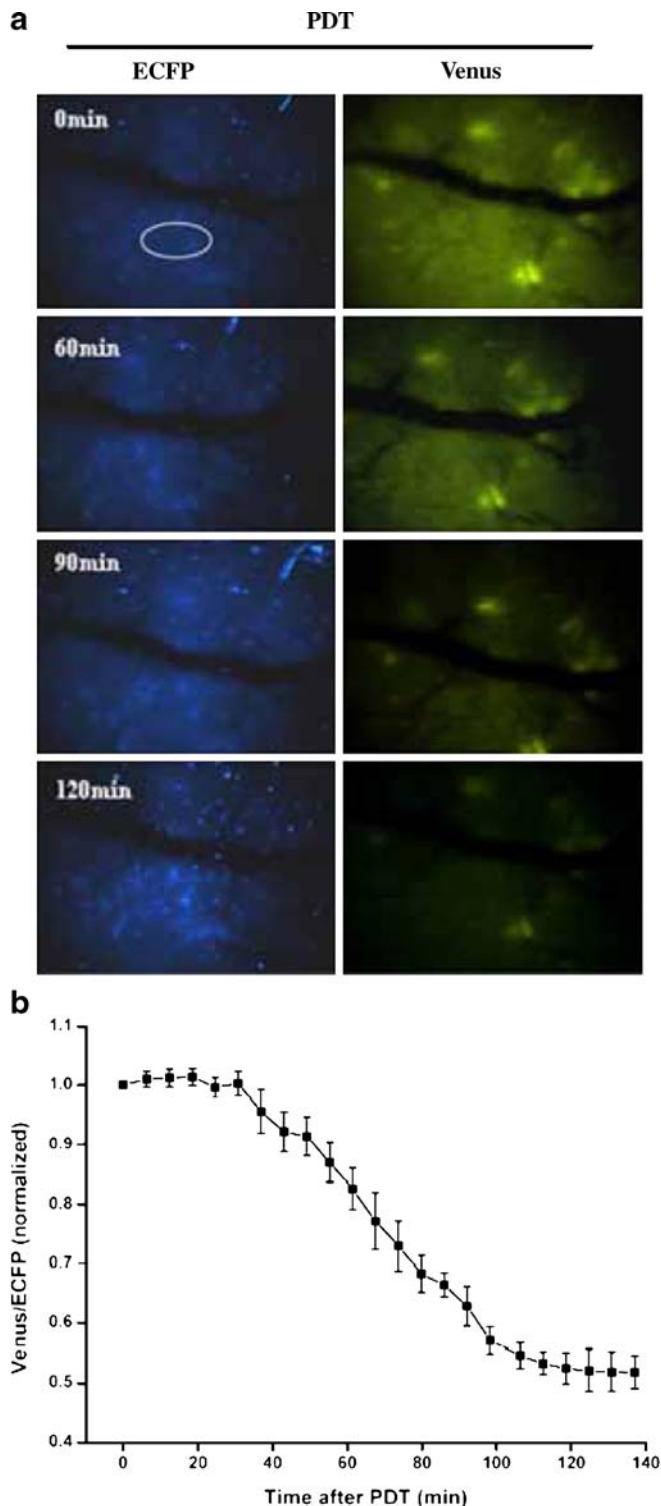
Real-time Detection of Caspase-3 Activation in Live Animals During Therapy

To ensure that the fluorescent signals of SCAT3-expressing tumors in mice were not biased by autofluorescence, we compared images of the mouse tumors established using cells with or without SCAT3 transfection. The fluorescent signals of SCAT3-expressing tumors in mice were much stronger than that of the autofluorescence from non-transfected tumors (Fig. 3). As a control, ECFP and Venus fluorescent images were obtained from a SCAT3-expressing tumor sample without treatment at 0, 24, 36, and 48 h, starting on day 7 of tumor cell inoculation (Fig. 4a). The time course of the Venus/ECFP fluorescence intensity ratio obtained from four ROIs is given in Fig. 4b. The fluorescent emission from the SCAT3-expressing tumor sample remained constant during the entire observation period of 48 h (Fig. 4). The results indicated that without external intervention (PDT or cisplatin, in this study), FRET efficiency was stable and caspase-3 was not activated *in vivo*.

After PDT therapy treatment of mouse tumors, ECFP and Venus fluorescent images were obtained at 0, 60, 90, and 120 min (Fig. 5a). The time course of the Venus/ECFP fluorescence intensity ratio obtained from four ROIs is given in Fig. 5b. The Venus/ECFP fluorescence intensity ratio started decreasing about 30 min after the PDT treatment and reached a stable level after about 70 min (Fig. 5b).

Immediately after the last administration of cisplatin, the ECFP and Venus fluorescent images of the treated mouse tumors were obtained at 0, 38, 40, and 42 h (Fig. 6a). The time course of the Venus/ECFP fluorescence intensity ratio obtained from four ROIs is given in Fig. 6b. The changes of fluorescence intensities of ECFP and Venus started much later, compared with the PDT treatment. The ECFP/Venus ratio started decreasing about 36 h after the cisplatin treatment and took about 4 h to reach a stable level (Fig. 6b).

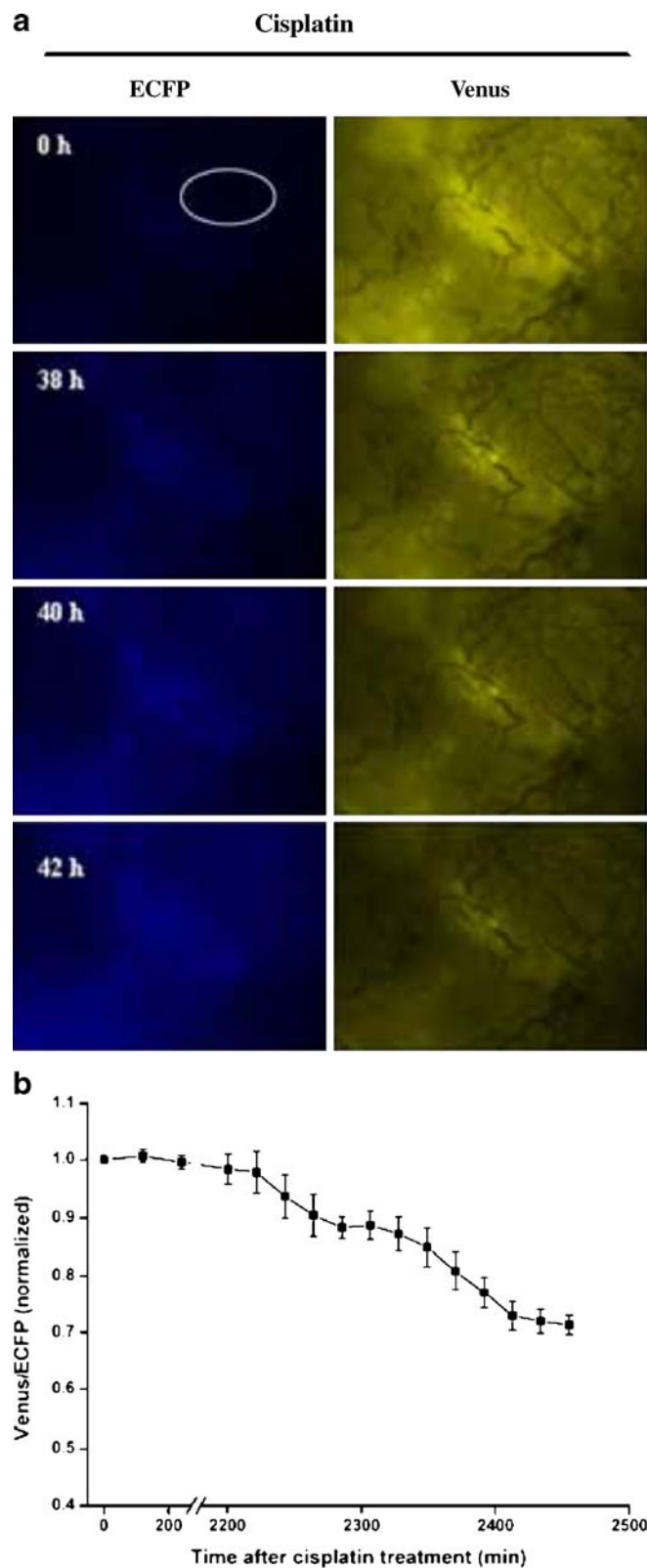
These results demonstrated that caspase-3 was activated to cleave the linker of SCAT3, DEVD, thus disrupting the FRET during apoptosis induced by PDT or cisplatin.



Discussion

Photodynamic therapy and chemotherapeutic drugs are widely used for cancer treatment. Noninvasive imaging of cell death in tumors can provide a means of accurate

Fig. 6. Dynamics of caspase-3 activation in a mouse tumor after cisplatin therapy. **a** Fluorescent images of ECFP and Venus from a mouse tumor at 0, 38, 40, and 42 h after cisplatin treatment. **b** Time course of the Venus/ECFP fluorescence intensity ratio obtained from four ROIs of the mouse tumor after cisplatin treatment. On day 7 after inoculation with tumor cells stably expressing SCAT3, animals received daily i.p. injections of cisplatin (10 mg/kg in 100 μ l) for five consecutive days. The fluorescent images and intensities of ECFP and Venus emission were acquired by the fluorescence stereo microscope, immediately after the last cisplatin injection.



assessment of the tumor response to anti-tumor treatments. It has been demonstrated that FRET can be used for imaging apoptosis in single cells [20–25, 29, 30–32]. In this study, using FRET, activation of caspase-3 was observed as one biomarker to monitor *in vivo* tumor cell apoptosis induced by different treatments. The caspase-3 activation was clearly demonstrated by the decrease of FRET in treated cells (Fig. 1b–d). Tumors in animals established with cells stably expressing SCAT3 provided FRET signals that could be quantified using a commercial fluorescence stereo microscope (Fig. 3). With appropriate selection of treatment protocol and observation period in our experiments, SCAT3 remained fluorescent in the tumor cells during the therapy and the observation (Figs. 4, 5, and 6). Therefore, the SCAT3 probes did not depend on any reagents and the use of SCAT3 could avoid additional administration like many other genetically encoded optical probes.

It should be pointed out that this approach is applicable to the tumors with significant caspase-3 activation. In other cases, different biomarkers should be used for *in vivo* monitoring of treatment effects.

It should be noted that different environments (*in vitro* and *in vivo*) and different treatments (PDT and cisplatin) had resulted in different dynamics of caspase-3 activation, as shown in Figs. 1c, d, 5b, and 6b. However, the ratio reduction and the final level of the Venus/ECFP emission ratio in each case clearly demonstrated the effects of PDT and cisplatin in activating intracellular caspase-3 to cleave the linker of SCAT3, DEVD, thus disrupting the FRET during the induced apoptosis.

In conclusion, with a recombinant FRET probe, we have detected the caspase-3 activation in live animals during different tumor treatments. We demonstrated that the modulation of cell death induced by PDT and cisplatin could be assessed using an optical method. By choosing appropriate recombinant substrates as probes, FRET can be potentially used in real-time to study the mechanism of tumor therapy.

Acknowledgements. This research is supported by the National Natural Science Foundation of China (30627003;30870676;3087065), the Natural Science Foundation of Guangdong Province (7117865), and by a grant from the US National Institute of Health (P20 RR016478 from the INBRE Program of the National Center for Research Resources).

References

- Ashkenazi A, Dixit VM (1998) Death receptors: signaling and modulation. *Science* 281:1305–1308
- Nagata S (1997) Apoptosis by death factor. *Cell* 88:355–365
- Chinnaiyan AM, Prasad U, Shankar S, Hamstra DA, Shanaiah M, Chenevert TL, Ross BD, Rehemtulla A (2000) Combined effect of tumor necrosis factor-related apoptosis-inducing ligand and ionizing radiation in breast cancer therapy. *Proc Natl Acad Sci U S A* 97:1754–1759
- Blankenberg FG, Katsikis PD, Storrs RW, Beaulieu C, Spielman D, Chen JY, Naumovski L, Tait JF (1997) Quantitative analysis of apoptotic cell death using proton nuclear magnetic resonance spectroscopy. *Blood* 89:3778–3786
- Aboagye EO, Bhujwala ZM, Shungu DC, Glickson JD (1998) Detection of tumor response to chemotherapy by ^1H nuclear magnetic resonance spectroscopy: effect of 5-fluorouracil on lactate levels in radiation-induced fibrosarcoma 1 tumors. *Cancer Res* 58:1063–1067
- Evelhoch JL, Gillies RJ, Karczmar GS, Koutcher JA, Maxwell RJ, Nalcioglu O, Raghunand N, Ronen SM, Ross BD, Swartz HM (2000) Applications of magnetic resonance in model systems: cancer therapeutics. *Neoplasia* 2:152–165
- Laxman B, Hall DE, Bhojani MS, Hamstra DA, Chenevert TL, Ross BD, Rehemtulla A (2002) Noninvasive real-time imaging of apoptosis. *Proc Natl Acad Sci U S A* 99:16551–16555
- Kanno A, Ozawa T, Umezawa Y (2006) Genetically encoded optical probe for detecting release of proteins from mitochondria toward cytosol in living cells and mammals. *Anal Chem* 78:8076–8081
- Ntzachristos V, Schellenberger EA, Ripoll J, Yessayan D, Graves E, Bogdanov A, Josephson L, Weissleder R (2004) Visualization of antitumor treatment by means of fluorescence molecular tomography with an annexin V–Cy5.5 conjugate. *Proc Natl Acad Sci U S A* 101:12294–12299
- Petrovsky A, Schellenberger E, Josephson L, Weissleder R, Bogdanov A (2003) Near-infrared fluorescent imaging of tumor apoptosis. *Cancer Res* 63:1936–1942
- Messerli S, Prabhakar S, Tang Y, Shah K, Cortes M, Murthy V, Weissleder R, Breakefield XO, Tung CH (2004) A novel method for imaging apoptosis using a caspase-1 near-infrared fluorescent probe. *Neoplasia* 6(2):95–105
- Bullock KE, Maxwell D, Kesarwala AH, Gammon S, Prior JL, Snow M, Stanley S, Piwnicka-Worms D (2007) Biochemical and *in vivo* characterization of a small, membrane-permeant, caspase-activatable far-red fluorescent peptide for imaging apoptosis. *Biochemistry* 46(13):4055–4065
- Hara M, Bindokas V, Lopez JP, Kaihara K, Landa LR, Harbeck M, Roe MW (2004) Imaging endoplasmic reticulum calcium with a fluorescent biosensor in transgenic mice. *Am J Physiol Cell Physiol* 287:C932–C938
- Bartoli M, Bourg N, Stockholm D, Raynaud F, Delevacque A, Han Y, Borel P, Seddik K, Armande N, Richard I (2006) A mouse model for monitoring calpain activity under physiological and pathological conditions. *J Biol Chem* 281:39672–39680
- Bins AD, van Rheenen J, Jalink K, Halstead JR, Divecha N, Spencer DM, Haanen JBAG, Schumacher TNM (2007) Intravital imaging of fluorescence markers and FRET probes by DNA tattooing. *BMC Biotechnol* 7:2
- Fadok VA, Henson PM (1998) Apoptosis: getting rid of the bodies. *Curr Biol* 8:R693–695
- Ting AY, Kain KH, Klemke RL, Tsien RY (2001) Genetically encoded fluorescent reporters of protein tyrosine kinase activities in living cells. *Proc Natl Acad Sci U S A* 98:15003–15008
- Zhang J, Campbell RE, Ting AY, Tsien RY (2002) Creating new fluorescent probes for cell biology. *Nat Rev Mol Cell Biol* 3:906–918
- Sekar RB, Periasamy A (2003) Fluorescence resonance energy transfer (FRET) microscopy imaging of live cell protein localizations. *J Cell Biol* 160:629–633
- Gao XJ, Chen TS, Xing D, Wang F, Pei YH, Wei XB (2006) Single cell analysis of PKC activation during proliferation and apoptosis induced by laser irradiation. *J Cell Phys* 206:441–448
- Ward MW, Rehm M, Duesmann H, Kacmar S, Concannon CG, Prehn JHM (2006) Real time single cell analysis of bid cleavage and bid translocation during caspase-dependent and neuronal caspase-independent apoptosis. *J Biol Chem* 281:5837–5844
- Rehm M, Duesmann H, Janicke RU, Tavare JM, Kogel D, Prehn JHM (2002) Single-cell fluorescence resonance energy transfer analysis demonstrates that caspase activation during apoptosis is a rapid process. *J Biol Chem* 277:24506–24514
- Luo KQ, Yu VC, Pu Y, Chang DC (2001) Application of the fluorescence resonance energy transfer method for studying the dynamics of caspase-3 activation during UV-induced apoptosis in living HeLa cells. *Biochem Biophys Res Commun* 283:1054–1060
- Thorburn J, Bender LM, Morgan MJ, Thorburn A (2003) Caspase- and serine protease-dependent apoptosis by the death domain of FADD in normal epithelial cells. *Mol Biol Cell* 14:67–77
- Nagai T, Yamada S, Tominaga T, Ichikawa M, Miyawaki A (2004) Expanded dynamic range of fluorescent indicators for Ca^{2+} by circularly permuted yellow fluorescent proteins. *Proc Natl Acad Sci U S A* 101:10554–10559
- Miyawaki A, Llopis J, Heim R, McCaffery JM, Adams JA, Ikura M, Tsien RY (1997) Fluorescent indicators for Ca^{2+} based on green fluorescent proteins and calmodulin. *Nature* 388:882–887
- Takemoto K, Nagai T, Miyawaki A, Miura M (2003) Spatiotemporal activation of caspase revealed by indicator that is insensitive to environmental effects. *J Cell Biol* 160:235–243
- Tyas L, Brophy VA, Pope A, Rivett AJ, Tavare JM (2000) Rapid caspase-3 activation during apoptosis revealed using fluorescence-resonance energy transfer. *Eur Mol Biol Org Rep* 1:266–270
- Wu YX, Xing D, Luo SM, Tang YH, Chen Q (2006) Detection of caspase-3 activation in single cells by fluorescence resonance energy transfer during photodynamic therapy induced apoptosis. *Cancer Lett* 235:239–247
- Wang F, Chen TS, Xing D, Wang JJ, Wu YX (2005) Measuring dynamics of caspase-3 activity in living cells using FRET technique during apoptosis induced by high fluence low-power laser irradiation. *Lasers Surg Med* 36:2–7
- Xue L, Chiu S, Oleinick NL (2001) Photodynamic therapy induced death of MCF-70 human breast cancer cells: a role for caspase-3 in the late steps of apoptosis but not for the critical lethal event. *Exp Cell Res* 263:145–155
- Li Y, Xing D, Chen Q (2009) Dynamic monitoring of apoptosis in chemotherapies with multiple fluorescence reporters. *Mol Imaging Biol* 11:213–222